Topological insulator and quantum memory

M. Kulig,[1] P. Kurashvili,[2] C. Jasiukiewicz,[1] M. Inglot,[1] S. Wolski,[1] S. Stagraczyński,[3] T. Masłowski,[1] T. Szczepański,[1] R. Stagraczyński,[1] V. K. Dugaev,[1] and L. Chotorlishvili[1]

[1]*Department of Physics and Medical Engineering, Rzeszów University of Technology, 35-959 Rzeszów, Poland*

[2]*National Centre for Nuclear Research, Warsaw 00-681, Poland*

[3]*Institute of Spintronics and Quantum Information, Faculty of Physics, Adam Mickiewicz University, 61-614 Poznań, Poland*

(Received 19 June 2023; revised 17 August 2023; accepted 21 September 2023; published 10 October 2023)

Measurements performed on quantum systems are too specific. Unlike their classical counterparts, quantum measurements can be invasive and destroy the state of interest. Besides, quantumness limits the accuracy of measurements performed on quantum systems. Uncertainty relations define the universal accuracy limit of the quantum measurements. Relatively recently, it was discovered that quantum correlations and quantum memory might reduce the uncertainty of quantum measurements. In this paper, we study two different types of measurements performed on the topological system. Namely, we discuss measurements performed on the spin operators and measurements performed on the canonical pair of operators: momentum and coordinate. We quantify the spin operator's measurements through the entropic measures of uncertainty and exploit the concept of quantum memory. In contrast, for the momentum and coordinate operators, we exploit the improved uncertainty relations. We discover that quantum memory reduces the uncertainties of spin measurements. On the other hand, we prove that the uncertainties in the measurements of the coordinate and momentum operators depend on the value of the momentum and are substantially enhanced at small distances between itinerant and localized electrons (the large-momentum limit). We note that the topological nature of the system leads to the spin-momentum locking. The momentum of the electron depends on the spin, and vice versa. Therefore we suggest an indirect measurement scheme for the momentum and coordinate operators through the spin operator. Due to the factor of quantum memory, such indirect measurements in topological insulators have smaller uncertainties than direct measurements.

DOI: 10.1103/PhysRevB.108.134411

I. INTRODUCTION

Heisenberg's uncertainty principle limits the precision of measurements performed on momentum $\hat{p}$ and coordinate $\hat{x}$ of a quantum particle; that is, pinpoint measurement of one of the variables enhances uncertainty about the second variable, and vice versa: $\Delta x \Delta p \geqslant \hbar$, where $\hbar$ is Planck's constant [1]. Note that from the point of view of classical mechanics, the momentum and coordinate are a pair of canonical variables. From the point of view of quantum mechanics, momentum and coordinate operators violate commutativity $[\hat{p}, \hat{x}] \neq 0$, i.e., the property of two operators considered together. Commutativity applies also to a broader class of Hermitian operators which are not canonically conjugate. The generalization of Heisenberg's uncertainty principle by Robertson applies to two arbitrary operators $\hat{A}$ and $\hat{B}$ and has the form [2]

$$\Delta A \cdot \Delta B \geqslant \tfrac{1}{2} |\langle\psi| [\hat{A}, \hat{B}] |\psi\rangle|, \tag{1}$$

where $\Delta O = \sqrt{\langle \hat{O}^2 \rangle - \langle \hat{O} \rangle^2}$. While Eq. (1) is more general than Heisenberg's relation, it still depends on the choice of the state over which averaging is performed. Consequently, when the state $|\psi\rangle$ is the eigenfunction of one of the operators $\hat{A}$ or $\hat{B}$, Eq. (1) takes a trivial form. Maccone and Pati tried to avoid this problem and quantified uncertainty through two orthogonal states as follows [3]:

$$\Delta A^2 + \Delta B^2 \geqslant i \langle\psi| [\hat{A}, \hat{B}] |\psi\rangle + |\langle\psi| \hat{A} + i\hat{B} |\psi^{\perp}\rangle|^2. \tag{2}$$

Here, $|\psi^{\perp}\rangle$ is the state orthogonal to $|\psi\rangle$. The early attempts at studying quantum uncertainty relations concerned a proper choice of quantum states. However, remarkable recent progress was achieved through reforming the uncertainty paradigm to the entropic measures and entropic uncertainty relations. We admit a celebrated work [4]. The core concepts of entropic uncertainty relations are viable for quantum guessing games and quantum memory [5–14].

In what follows, we study a guessing game between two parties Alice (A) and Bob (B). We implement tools of quantum metrology to the experimentally feasible condensed matter system: a quantum dot placed on the surface of a topological insulator (TI). The model of interest is described in the next section in detail. Here we specify the rules of the quantum game that has to be played. In the quantum game, Bob represents a quantum dot (QD) placed on the surface of a TI. Bob selects a single electron A from the surface of the TI and scatters electron A on the electron B localized in the QD. Bob shares the scattered electron A with Alice and lets her perform two consecutive measurements on A. Alice performs two measurements on the spin A. In the first measurement, Alice measures the Z component of the spin, and in the second measurement she measures the X component. Alice denotes a set of measurements performed on A by $R \equiv \{Z, X\}$ and stores measurement results in L. The aim of Bob is to guess the results of the measurements $R \equiv \{Z, X\}$. Bob's uncertainty about the measurements' result can be reduced by quantum

memory. We note that these types of measurements are quite important for spintronics [15,16]. In this paper, we analyze two types of measurements performed on the system: measurements performed on the momentum and coordinate of the itinerant electron and spin projections of the itinerant electron. To explore uncertainties of the measurements performed on the momentum and coordinate, we follow Maccone and Pati [3]. When quantifying uncertainties of the spin measurements, we exploit the quantum memory. In the first case, we show that uncertainty increases with the momentum k (i.e., at the shorter distances between localized and itinerant electrons). On the other hand, the spin measurements' uncertainty is reduced by the quantum memory and is independent of k. The paper is organized as follows: In Sec. II, we describe the model. In Sec. III, we describe uncertainties of the momentum and coordinate measurements. In Sec. IV, we analyze entropic measures of spin measurements and quantum memory. In Sec. V we conclude the work.

II. MODEL

The system in which we are interested consists of a two-dimensional (2D) surface itinerant electron in a topological insulator $\hat{H}_I$, a localized electron in a quantum dot placed on the surface of the topological insulator $\hat{H}_D$, and the exchange interaction $\hat{V}$ between itinerant and localized electrons:

$$\hat{H}_{\rm tot} = \hat{H}_I + \hat{H}_D + \hat{V}. \tag{3}$$

The Hamiltonian of the surface electron explicitly reads as follows [17]: $\hat{H}_I = -iv\,\hat{\boldsymbol{\sigma}}_A \cdot \boldsymbol{\nabla}$, where $\hat{\boldsymbol{\sigma}}_A = (\hat{\sigma}_x, \hat{\sigma}_y, 0)$ and $\hat{\sigma}_x, \hat{\sigma}_y$ are Pauli matrices and v is the velocity of the surface electron. The eigenstates and eigenenergies of the surface electrons can be found easily: $\psi_{T,\sigma}(\mathbf{r}) = \frac{e^{i\mathbf{k}\cdot\mathbf{r}}}{\sqrt{2}}\binom{1}{\pm k_+/k}$, $E = \pm vk$, where $k_+ = k_x + ik_y$, $k = \sqrt{k_x^2 + k_y^2}$, and $\mathbf{r} = (x, y)$. The Hamiltonian of the electron localized in the quantum dot (QD) has the form

$$\hat{H}_D = -B\hat{\sigma}_B^z - \frac{\hbar^2}{2m}\vec{\nabla}^2 + \frac{1}{2}m\omega_0^2 r^2, \tag{4}$$

where ω_0 is the frequency of electron oscillation in the QD. Through the external magnetic field applied locally to the quantum dot (e.g., through spin-polarized scanning tunneling microscopy (SP-STM) [18,19]), we can freeze (strong field) or relax the spin of the localized electron $\hat{\sigma}_B^z$ depending on the value of Zeeman splitting $B \equiv \hbar\gamma_e B$ (e.g., the direction of the spin is not rigorously fixed, and it is possible to perform gate operations on the spin). The lowest eigenstate of the localized electron has the form

$$\psi_D(\mathbf{r}) = \frac{1}{l_B\sqrt{\pi}}\exp\left(-\frac{x^2+y^2}{2l_B^2}\right),$$
$$l_B^2 = l_0^2/\sqrt{1 + B^2e^2l_0^4/4\hbar^2}. \tag{5}$$

Here, $l_0 = (\hbar/m\omega_0)^{1/2}$ is the confinement length [20]. The last term in Eq. (3) describes the interaction between localized and surface electrons $\hat{V} = J\,\hat{\boldsymbol{\sigma}}_A \cdot \hat{\boldsymbol{\sigma}}_B\,\delta(\mathbf{r}_1 - \mathbf{r}_2)$. The origin of the exchange interaction and exchange constant J is described in Ref. [21]. In what follows, $E \equiv \langle E\rangle = \langle vk\rangle$, and we set the dimensionless parameters through $\hat{H}_{\rm tot} \to \hat{H}_{\rm tot}/J$. Following the recent work [22], we consider the spin-dependent formulation of the scattering problem and exploit the Lippmann-Schwinger integral equation. When studying the scattering of the itinerant electron on the magnetic impurity, the impurity magnetic moment, in many cases, is assumed to be fixed. In contrast to that, we consider a case where both spins (itinerant electron and quantum dot) can flip. Therefore the postscattering wave function in our case should contain both projections of both spins. Considering conservation of the total spin, we apply the Lippmann-Schwinger approach formulated for the spin-dependent scattering problem [23]. The initial wave function is a product state $\psi_{T,\sigma}(\mathbf{r}_A) = \psi(\mathbf{r}_A)(\alpha|0\rangle_A + \beta|1\rangle_A)$ and $\psi_{D,\sigma}(\mathbf{r}_B) = \psi(\mathbf{r}_B)|0\rangle_B$, and for brevity, in what follows $\mathbf{r}_A \equiv \mathbf{r}_1$ and $\mathbf{r}_B \equiv \mathbf{r}_2$. Two states of the localized electron $\psi_{D,0}(\mathbf{r}) = \psi_D(\mathbf{r})|0\rangle$ (spin up, $|0\rangle \equiv |\uparrow\rangle$) and $\psi_{D,1}(\mathbf{r}) = \psi_D(\mathbf{r})|1\rangle$ (spin down, $|1\rangle \equiv |\downarrow\rangle$) with the respective energies ε_0 and $\varepsilon_1 = \varepsilon_0 + 2B$ (hereinafter, we set $\varepsilon_0 = 0$) contribute to the postscattering state. The postscattering wave function of the two-electron system reads as follows [22]: $\Psi_{\sigma_1\sigma_2}(\mathbf{r}_1, \mathbf{r}_2) = \psi_{T,0}^{(+)}(\mathbf{r}_1)\psi_{D,0}(\mathbf{r}_2) + \psi_{T,1}^{(+)}(\mathbf{r}_1)\psi_{D,1}(\mathbf{r}_2)$. In particular, we consider the following initial state of the itinerant electron: $\psi_{T,\sigma}(\mathbf{r}_A) = \psi(\mathbf{r}_A)|0\rangle_A$. Then the spinor $\psi_{T,0}^{(+)}(\mathbf{r})$ quantifies the contribution to the scattering process without flipping the spin, while the spinor $\psi_{T,1}^{(+)}(\mathbf{r})$ quantifies the contribution of the spin-flipping process. Both spinors $\psi_{T,0}^{(+)}(\mathbf{r}) = \binom{\phi_0(\mathbf{r})}{\chi_0(\mathbf{r})}$ and $\psi_{T,1}^{(+)}(\mathbf{r}) = \binom{\phi_1(\mathbf{r})}{\chi_1(\mathbf{r})}$ are found from the coupled integral equations

$$\begin{pmatrix}\phi_0(\mathbf{r})\\ \chi_0(\mathbf{r})\end{pmatrix} = \frac{e^{i\mathbf{kr}}}{\sqrt{2}}\begin{pmatrix}1\\ k_+/k\end{pmatrix} + \int d^2r'\,\hat{G}^{(+)}(\mathbf{r},\mathbf{r}';E)\hat{V}_{00}(\mathbf{r}')\begin{pmatrix}\phi_0(\mathbf{r}')\\ \chi_0(\mathbf{r}')\end{pmatrix} + \int d^2r'\,\hat{G}^{(+)}(\mathbf{r},\mathbf{r}';E)\hat{V}_{01}(\mathbf{r}')\begin{pmatrix}\phi_1(\mathbf{r}')\\ \chi_1(\mathbf{r}')\end{pmatrix},$$
$$\begin{pmatrix}\phi_1(\mathbf{r})\\ \chi_1(\mathbf{r})\end{pmatrix} = \int d^2r'\,\hat{G}^{(+)}(\mathbf{r},\mathbf{r}';E-2B)\hat{V}_{10}(\mathbf{r}')\begin{pmatrix}\phi_0(\mathbf{r}')\\ \chi_0(\mathbf{r}')\end{pmatrix} + \int d^2r'\,\hat{G}^{(+)}(\mathbf{r},\mathbf{r}';E-2B)\hat{V}_{11}(\mathbf{r}')\begin{pmatrix}\phi_1(\mathbf{r}')\\ \chi_1(\mathbf{r}')\end{pmatrix}, \tag{6}$$

where $E = vk$ is the energy of the itinerant electron, the Green's function is given by $\hat{G}^{(+)}(\mathbf{r},\mathbf{r}';E) = -\frac{E}{2\pi v^2}[K_0(-iE|\mathbf{r}-\mathbf{r}'|/v)\hat{I} + K_1(-iE|\mathbf{r}-\mathbf{r}'|/v)\hat{\sigma}^x]$, and $K_{0,1}$ are the modified Bessel functions (the Macdonald functions). We skip cumbersome details [22] of the solution of Eq. (6) and present the final result:

$$|\psi\rangle = C_1\,|0\rangle_A\,|0\rangle_B + C_2\,|0\rangle_A\,|1\rangle_B + C_3\,|1\rangle_A\,|0\rangle_B + C_4\,|1\rangle_A\,|1\rangle_B\,. \tag{7}$$

Here, we introduced the following notations:

$$C_1(\rho,\varphi) = \frac{\psi_D(\rho')}{2\pi\sqrt{2}C_0}(2\pi e^{ik\rho\cos\varphi} + k_J k(A_0(\rho,\varphi) + e^{i\theta}A_1(\rho,\varphi))),$$
$$C_2(\rho,\varphi) = -\frac{\psi_D(\rho')}{2\pi\sqrt{2}C_0}(2k_J(k-2k_B)A_{0B}(\rho,\varphi))e^{i\theta},$$
$$C_3(\rho,\varphi) = \frac{\psi_D(\rho')}{2\pi\sqrt{2}C_0}(2\pi e^{ik\rho\cos(\varphi)} + k_J k(A_0(\rho,\varphi) + e^{-i\theta}A_1(\rho,\varphi)))e^{i\theta},$$
$$C_4(\rho,\varphi) = -\frac{\psi_D(\rho')}{2\pi\sqrt{2}C_0}(2k_J(k-2k_B)A_{1B}(\rho,\varphi))e^{i\theta}, \quad (8)$$

where C_0 is chosen from the normalization condition $\sqrt{|C_1|^2+|C_2|^2+|C_3|^2+|C_4|^2}=1$, ϱ,φ are polar coordinates, and coefficients A are defined in Appendix A. Dimensionless parameters are introduced through the following notations: $k_+/k = e^{i\theta}$, $J/v = k_J$, $E \equiv E/J$, $E_B = E - 2B$, $E/v = k$, $E_B/v = k - 2k_B$, $k_B \equiv B/v$, and $l = 0, 1$. In the coefficients $A_{lB}(\mathbf{r})$, indices $l = 0, 1$ define the zeroth- and first-order modified Bessel functions and $B = 0, 1$ indicate the zero and nonzero magnetic field problems.

III. MOMENTUM AND COORDINATE UNCERTAINTIES

We apply the improved uncertainty relations by Maccone and Pati, Eq. (2), to our system. Following Refs. [1,24], we define the operators for the TI and QD as $\hat{p}_\rho = -i\hbar(\frac{d}{d\rho} + \frac{1}{\rho})$ and $\hat{p}_{\rho'} = -i\hbar(\frac{d}{d\rho'} + \frac{1}{\rho'})$ and obtain commutation relations $[\rho, \hat{p}_\rho] = i\hbar$, $[\rho', \hat{p}_{\rho'}] = i\hbar$, $[\rho^2, \hat{p}_\rho^2] = 4\hbar^2(\rho\frac{d}{d\rho} + \frac{3}{2})$, and $[\rho'^2, \hat{p}_{\rho'}^2] = 4\hbar^2(\rho'\frac{d}{d\rho'} + \frac{3}{2})$. The operator $\hat{p}_\varphi = -i\frac{\partial}{\partial\varphi}$ leads to the complications. It is Hermitian in the space of functions with a period of 2π. However, if we restrict discussion to this range, then commutation relations should be modified following Ref. [25], meaning that one has to include a series of δ functions:

$$[\hat{p}_\varphi, \varphi] = i\left\{1 - 2\pi\sum_{n=-\infty}^{+\infty}\delta[\varphi - (2n+1)\pi]\right\}. \quad (9)$$

In order to avoid complications with Eq. (9) we consider two cases [26,27] of the commutator $[\sin\varphi, \hat{p}_\varphi] = i\cos\varphi$ and consider the operators $\hat{S} = e^{i\varphi}$, $\hat{P} = \hat{S}\frac{\partial}{\partial\hat{S}}$, $[\hat{P}, \hat{S}] = \hat{S}$. We note that unlike the operator $\hat{p}_\varphi$, the operator $\hat{P}$ is Hermitian in the whole range of $\hat{S}$. Taking into account Eqs. (2), (7), and (8), after cumbersome calculations we deduce

$$\Delta P^2 + \Delta S^2 \geqslant i\langle\psi|[\hat{P},\hat{S}]|\psi\rangle + |\langle\psi|\hat{P} + i\hat{S}|\psi^\perp\rangle|^2,$$
$$\Delta(\sin\varphi)^2 + \Delta p_\varphi^2 \geqslant i\langle\psi|[\sin\varphi, \hat{p}_\varphi]|\psi\rangle + |\langle\psi|\sin\varphi + i\hat{p}_\varphi|\psi^\perp\rangle|^2,$$
$$\Delta p_\rho^2 + \Delta\rho^2 \geqslant i\langle\psi|[\hat{p}_\rho, \hat{\rho}]|\psi\rangle + |\langle\psi|\hat{p}_\rho + i\hat{\rho}|\psi^\perp\rangle|^2. \quad (10)$$

Applying Eq. (10) to realistic physical systems of interest technically is rather demanding. Therefore we calculate only one particular relation (hereinafter $\hbar = 1$):

$$\Delta p_\rho^2 + \Delta\rho^2 \geqslant 1 + \left|\langle\psi|\rho - \left(\frac{d}{d\rho} + \frac{1}{\rho}\right)|\psi^\perp\rangle\right|^2. \quad (11)$$

The set of the states $\mathbb{C} = \{\Psi^\perp\}$ orthogonal to $|\psi\rangle$ we express in terms of the coefficients from Eq. (8) as follows:

$$\Psi_1^\perp = \{C_2, -C_1, C_4, -C_3\}, \quad (12)$$
$$\Psi_2^\perp = \{C_3, -C_4, -C_1, C_2\}, \quad (13)$$
$$\Psi_3^\perp = \{C_4, -C_3, C_2, -C_1\}. \quad (14)$$

The general orthogonal wave function reads

$$|\psi^\perp\rangle = \sum_{i=b}^{3}\alpha_b|\Psi^\perp{}_b\rangle, \quad (15)$$

where $|\alpha_1|^2 + |\alpha_2|^2 + |\alpha_3|^2 = 1$. Then we rewrite the general orthogonal function in the computational basis of Eq. (7):

$$\psi^\perp = \sum C_i^\perp|\psi\rangle_{AB}. \quad (16)$$

The coefficients $C_i^\perp$ are expressed through the coefficients $\{C_i\}$ and parameters $\{\alpha\}$:

$$C_1^\perp = \alpha_1 C_2 + \alpha_2 C_3 + \alpha_3 C_4, \quad (17)$$
$$C_2^\perp = -\alpha_1 C_1 - \alpha_2 C_4 - \alpha_3 C_3, \quad (18)$$
$$C_3^\perp = \alpha_1 C_4 - \alpha_2 C_1 + \alpha_3 C_2, \quad (19)$$
$$C_4^\perp = -\alpha_1 C_3 + \alpha_2 C_2 - \alpha_3 C_1. \quad (20)$$

Let $\hat{R}$ be an arbitrary operator and $R_{ik} = \int C_i^*\hat{R}C_k\rho d\rho d\varphi$ be its matrix element. Then

$$\langle\psi|R|\psi^\perp\rangle = \alpha_1[R_{12} - R_{21} + R_{34} - R_{43}] + \alpha_2[R_{13} - R_{31} - R_{24} + R_{42}] + \alpha_3[R_{14} - R_{41} - R_{23} + R_{32}]. \quad (21)$$

Comparing Eq. (21) with Eq. (11), we can see that the right-hand side of Eq. (11) is larger than 1 only if $R_{ik} \neq R_{ki}$. Therefore the nonzero $\langle\psi|\rho - (d_\rho + 1/\rho)|\psi\rangle^\perp$ is granted by the non-Hermitian part in the operator $\hat{R}$. As shown in Appendix B, the functions A_{ib} in the expressions for the coefficients $C_i(\rho,\varphi)$ can be written as a product of functions of ρ and φ:

$$A_{lb}(\rho,\varphi) = f_{\lambda b}(\rho)g_b(\varphi). \quad (22)$$

The first index, $l = 0, 1$, arises from the expansion of the Bessel-Macdonald functions. In the following we use $\lambda = 1 - 4l^2$, which is equal to either 1 or -3. The parameter of the angular function, b, takes the values 0 and B for zero and nonzero magnetic field, respectively. We set $l_B = 1$ and obtain

$$f_{b\lambda}(\rho) = \frac{\pi}{8k_b^2}e^{ik_b\rho}\left(\frac{\lambda}{\rho^3} + \frac{8ik_b}{\rho^2}\right), \quad (23)$$
$$g_b(\varphi) = a_{0b} + a_{1b}\cos\varphi + a_{2b}\cos^2\varphi, \quad (24)$$

where $\lambda = 1 - 4l^2$, $a_{0b} = 1 - (k_{(b)}^2/2) - (i\sqrt{\pi}/2)k_{(b)}$, $a_{1b} = [k_{(b)} + i\sqrt{\pi}/2]k$, $a_{2b} = k^2/2$, and k_b is either k or $k - 2k_B$

depending on the absence or presence of the magnetic field. The integrals of the uncertainty relation have the form

$$\int \rho d\rho d\varphi A^*_{l_1 b_1}(\rho,\varphi)\frac{\partial}{\partial\rho}A_{l_2 b_2}(\rho,\varphi) = \int d\varphi g_{b_1}(\varphi)g_{b_2}(\varphi)\int \rho d\rho f_{\lambda_1 b_1}(\rho)\frac{d}{d\rho}f_{\lambda_2 b_2}(\rho) = I^{\varphi}_{b_1 b_2} I^{R}_{\lambda_1\lambda_2, b_1 b_2}. \tag{25}$$

The integration over the angular variable is rather straightforward and yields

$$I^{\varphi}_{b_1 b_2} = \int_0^{2\pi} d\varphi g^*_{b1}(\varphi) g_{b2}(\varphi) = 2\pi a^*_{0b_1} a_{0b_2} + \pi(a^*_{1b_1}a_{1b_2} + a^*_{0b_1}a_{2b_1} + a^*_{2b_1}a_{0b_2}) + \frac{3\pi}{4}a^*_{2b_2}a_{2b_2}. \tag{26}$$

In Appendix C we write explicitly the form of these integrals for all possible values of the magnetic field. The result of the radial integrations reads

$$I^{R}_{\lambda_1\lambda_2 b_1 b_2} = \int_1^{\infty} \rho d\rho f^*_{\lambda_1 b_1}(\rho)\frac{d}{d\rho}f_{\lambda_2 b_2}(\rho) = \left[\frac{\pi}{k_{b1}k_{b2}}\right]^2 \sum_{n=2}^{5} F_n i^n (-i\Delta k_b)^n \Gamma(-n, -i\Delta k_b), \tag{27}$$

where $k_{1,2b} = k - 2k_{b_{1,2}} = (E - 2b_{1,2})/v$, $\Delta k_{(b)} = k_{1b} - k_{2b} = 2(b_2 - b_1)/v$, $b_{1,2} = 0, B$, and the coefficients F_n are

$$F_2 = k_{1b}k^2_{2b}, \tag{28}$$

$$F_3 = \frac{1}{8}\lambda_1 k^2_{2b} - \frac{1}{8}\lambda_2 k_{1b}k_{2b} + 2k_{1b}k_{2b}, \tag{29}$$

$$F_4 = \frac{1}{64}\lambda_1\lambda_2 k_{2b}, \tag{30}$$

$$F_5 = \frac{\lambda_1\lambda_2}{32}. \tag{31}$$

$\lambda_{0,1} = 1 - 4l^2_{0,1}$ can take on values of either 1 ($l = 0$) or -3 ($l = 1$).

The incomplete gamma functions with a negative integer index, $\Gamma(-n, x)$, satisfy the following condition in the limit $x \to \infty$:

$$\lim_{x\to 0} x^n \Gamma(-n, x) = \frac{1}{n}. \tag{32}$$

In Appendix D, we also calculate the sum of squares of the absolute values of the coefficients C_i truncating the contribution from the plane waves. We proceed to the uncertainty relation in Eq. (21). The simplest case corresponds to $\alpha_1 = 0, \alpha_2 = 1, \alpha_3 = 0$. Then, we calculate the differences between matrix elements $R_{13} - R_{31}$ and $R_{24} - R_{42}$, where $\hat{R}$ corresponds to the differentiation by ρ. Then antisymmetric combinations of the matrix elements read

$$R_{13} - R_{31} = \int \rho d\rho d\varphi \left[C^*_1\frac{d}{d\rho}C_3 - C^*_3\frac{d}{d\rho}C_1\right] = -2iA_{13}\left(I^R_{11,00}\sin 2\theta + \sin\theta\left[I^R_{10,00} + I^R_{01,00}\right]\right)I^{\varphi}_{00}, \tag{33}$$

$$R_{24} - R_{42} = 4A_{24}\left(I^R_{01,BB} - I^R_{10,BB}\right)I^{\varphi}_{BB}, \tag{34}$$

where

$$A_{13} = \frac{|\psi_D(\rho')|^2 k^2_J k^2}{8\pi^2|C_0|^2}, \tag{35}$$

$$A_{24} = \frac{|\psi_D(\rho')|^2 k^2_J (k - 2k_B)^2}{8\pi^2|C_0|^2}. \tag{36}$$

We write down the integrals from Eqs. (33) and (34). The results of the angular integrations I^{φ}_{00} and I^{φ}_{BB} are presented in Eqs. (C1) and (C2) of Appendix C. For radial integrals, we have

$$I^R_{11,00} = -\frac{\pi^2}{k^2}\left[\frac{k}{2}\left(k^2 - \frac{1}{128}\right) + i\left(\frac{2}{3}k^2 - \frac{1}{160}\right)\right], \tag{37}$$

$$I^R_{10,00} + I^R_{01,00} = -\frac{\pi^2}{k^2}\left[k\left(k^2 + \frac{1}{128}\right) + i\left(\frac{k^2}{3} + \frac{3}{80}\right)\right], \tag{38}$$

$$I^R_{10,BB} - I^R_{01,BB} = 0. \tag{39}$$

We see that for the transverse wave function of our choice, only the term $R_{13} - R_{31}$ given by Eq. (33) contributes to the uncertainty relation. Summarizing the obtained results, the entire expression of the uncertainty reads

$$\Delta p^2_\rho + \Delta\rho^2 \geqslant 1 + \left|\langle\psi|\frac{d}{d\rho}|\psi^{\perp}\rangle\right|^2 = 1 + \left|\int \rho d\rho d\varphi\left[C^*_1\frac{d}{d\rho}C_3 - C^*_3\frac{d}{d\rho}C_1 + C^*_2\frac{d}{d\rho}C_4 - C^*_4\frac{d}{d\rho}C_2\right]\right|^2. \tag{40}$$

The coefficients C_i are similar to those given in Eq. (7) without the contribution from the plane-wave components (the first terms inside the parentheses in the expressions for C_1 and C_3). In this case, C_0 is normalized by means of integration over the entire space, as discussed in Appendix D. The coefficient $|C_0|^2$ is equal to

$$|C_0|^2 = \frac{|\psi_D(\rho')|^2}{4}k^2_J \times\left[\frac{I^{\varphi}_{00}}{k^2}\left(k^2(1+\cos\theta) - \frac{1}{32}(1+2\cos\theta)\right) + \frac{I^{\varphi}_{BB}}{(k-2k_B)^2}\left((k-2k_B)^2 - \frac{1}{32}\right)\right]. \tag{41}$$

The coefficients I^{φ}_{00} and I^{φ}_{BB} arise from the angular integration of $A_{lb}(\rho,\varphi)$ and are written explicitly in Eqs. (C1) and (C2). The integrals of the radial part are expressed in terms of incomplete gamma functions, and it can be proved that in Eq. (40) only the first two terms, $C^*_1\frac{d}{d\rho}C_3$ and $C^*_3\frac{d}{d\rho}C_1$, contribute to the uncertainty. Without the normalization factors, those terms are equal to the sum of two terms proportional to $\sin 2\theta$ and $\sin\theta$, respectively [see Eq. (33)], and the values of the coefficients are given in Eqs. (37) and (38). In this approximation, dependence on the magnetic field in the form of k_B remains only in one of the normalization constants, C_0. To express our results in graphical form, we consider the

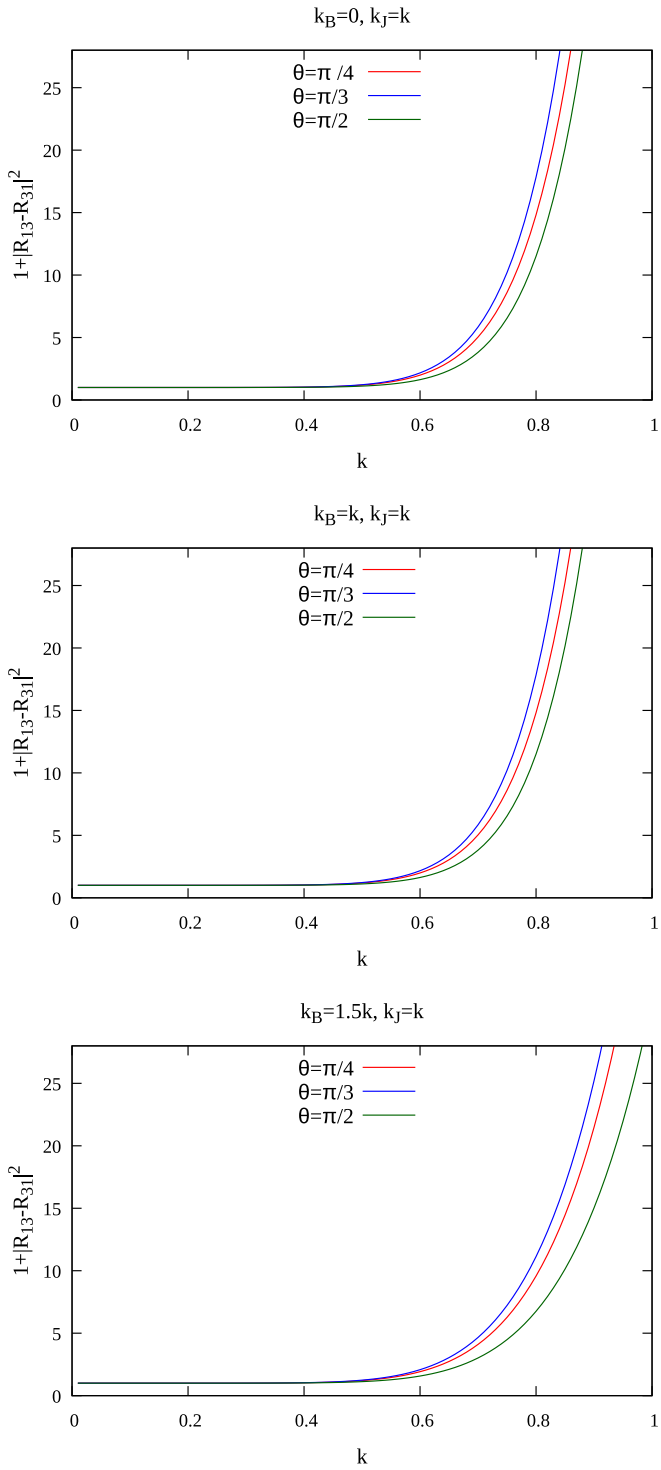

FIG. 1. Dependencies of the minimum value of the uncertainty relation as calculated from Eq. (40) for different coefficients of proportionality between k_B and k at fixed $k_J = k$ and three different values of θ.

center of the localized electron $\rho' = 0$, and $|\psi_D(\rho')|^2 = 1$. In Fig. 1, we plot the right-hand side of Eq. (40). Values above 1 are related to the contribution from the term $|\int [C_1^* \frac{d}{d\rho} C_3 - C_3^* \frac{d}{d\rho} C_1 + C_2^* \frac{d}{d\rho} C_4 - C_4^* \frac{d}{d\rho} C_2]|^2$. As we see, the uncertainty depends on the scattering angle and magnetic field. In the case of a strong magnetic field, $k_B = 1.5k$, uncertainty is smaller. On the other hand, uncertainty increases with the momentum $\mathbf{p} = \hbar\mathbf{k}$ (uncertainty is stronger at smaller distances). In what follows, we show that this is not the case for the quantum memory and entropic measures of the uncertainty.

IV. QUANTUM GUESSING GAME

Before starting the quantum guessing game between Alice and Bob, sharing the system of the TI and QD, we define quantities of interest and tools. Taking into account the wave function of the system $|\psi\rangle_{AB}$, we construct the density matrix $\hat{\varrho}_{AB} = |\psi\rangle\langle\psi|_{AB}$. Then, the reduced density matrices of the TI and QD subsystems are defined as follows: $\hat{\varrho}_A = \mathrm{Tr}_B(\hat{\varrho}_{AB})$ and $\hat{\varrho}_B = \mathrm{Tr}_A(\hat{\varrho}_{AB})$. The von Neumann entropy of the entire system is given by $S(AB) = -\mathrm{Tr}(\hat{\varrho}_{AB} \log_2 \hat{\varrho}_{AB})$. The conditional quantum entropy has the form $S(A|B) = S(AB) - S(B)$. After Alice performs two measurements and measures the z and x components of her qubit A, the subsequent postmeasurement density matrices are given through

$$\hat{\varrho}_{Z,AB} = \sum_n |\psi_n\rangle\langle\psi_n|_A \otimes \mathrm{Tr}_A\{(|\psi_n\rangle\langle\psi_n|_A \otimes \hat{I}_B)\hat{\varrho}_{AB}\}, \quad (42)$$

$$\hat{\varrho}_{X,AB} = \sum_n |\phi_n\rangle\langle\phi_n|_A \otimes \mathrm{Tr}_A\{(|\phi_n\rangle\langle\phi_n|_A \otimes \hat{I}_B)\hat{\varrho}_{AB}\}. \quad (43)$$

Here, $|\psi_{1,2}\rangle \equiv |0\rangle_A, |1\rangle_A$ and $|\phi_{1,2}\rangle = \frac{1}{\sqrt{2}}(|0\rangle_A \pm |1\rangle_A)$ are eigenfunctions of the z and x components of the qubit A.

Through the scattering process, Bob entangles the particle B QD with the particle A TI. Alice performs two measurements on her particle A and broadcasts her measurement choice to Bob. Bob wants to guess Alice's outcome precisely by measuring his particle B with the help of the received classical information (i.e., Alice's choice of measurement). Bob's ignorance about Alice's measurements is given by [4,28]

$$S(X|B) + S(Z|B) \geqslant \log_2(1/c) + S(A|B), \quad (44)$$

$$c_{ij} = \max\{|\langle\psi_i|\,|\phi_j\rangle|^2\}. \quad (45)$$

c is a measure of complimentarity.

In essence, this scheme allows one to read out information about the quantum dot through the measurements performed on the itinerant electron from the topological insulator, or vice versa, depending on the experimental feasibility and convenience. We briefly explain the meaning of Eqs. (44) and (45). The left-hand side of Eq. (44) defines the uncertainty about the measurement results (two measurements performed on the x and z spin components of the particle A). The right-hand side of Eq. (44) defines the lower bound of this uncertainty. The first term on the right-hand side, $\log_2(1/c)$, is positive. However, the conditional quantum entropy $S(A|B)$ can be negative for entangled states, and when it is negative, it reduces the lower bound of uncertainty. Negative conditional quantum entropy $S(A|B)$ means that the state $\hat{\varrho}_{AB}$ for sure is entangled, but the converse is not always true. As an example, one can consider the maximally entangled Bell state $\hat{\rho}_{AB} = |\Phi\rangle\langle\Phi|$, $|\Phi\rangle = \frac{1}{\sqrt{2}}(|0\rangle_A \otimes |0\rangle_B + |1\rangle_A \otimes |1\rangle_B)$. Then it is easy to see that $\log_2(1/c) = 1$, $S(A|B) = -1$, and the uncertainty is zero: $S(X|B) + S(Z|B) = 0$.

The density operator of our system $\hat{\varrho}_{AB}$ we present in the form

$$\hat{\varrho}_{AB} = \sum_{iklm} \rho_{iklm} \left|\psi_i^A \psi_k^B\right\rangle \left\langle \psi_l^A \psi_m^B\right| . \tag{46}$$

The indices $\{iklm\}$ run over the components of the basis states of the spins belonging to Alice and Bob meaning that each $|\psi_i^A\rangle \equiv |0\rangle^A, |1\rangle^A$ and the same for B. The matrix elements ρ_{iklm} are obtained from the coefficients C_i in Eq. (7):

$$\rho_{iklm} = C_{2i+k+1} C^*_{2l+m+1} = c_{ik} c^*_{lm}, \tag{47}$$

where $c_{00} = C_1$, $c_{01} = C_2$, $c_{10} = C_3$, and $c_{11} = C_4$. After inserting Eq. (46) into Eqs. (42) and (43), we deduce

$$\hat{\varrho}_{Z,AB} = \sum_{ikm} \rho_{ikim} \left|\psi_i^A \psi_k^B\right\rangle \left\langle \psi_i^A \psi_m^B\right| , \tag{48}$$

$$\hat{\varrho}_{X,AB} = \sum_{ikm} \rho^{(\Phi)}_{ikim} \left|\phi_i^A \phi_k^B\right\rangle \left\langle \phi_i^A \phi_m^B\right| , \tag{49}$$

where $\rho^{\Phi}_{\{i\}}$ are the matrix coefficients in the basis $\{\phi_1, \phi_2\}$. In order to calculate $\rho^{\Phi}_{\{i\}}$ we exploited Eqs. (7) and (47) and the coefficients $C_i^{(\Phi)}$ in the X basis. The details of the derivations are given in Appendix E.

We write down the explicit expressions of the reduced density operators:

$$\hat{\varrho}_A = \sum_{ik} \rho_{ik} \left|\psi_i^A\right\rangle \left\langle \psi_k^A\right| , \quad \rho_{ik} = \sum_m c_{im} c^*_{km}, \tag{50}$$

$$\hat{\varrho}_B = \sum_{ik} \rho_{ik} \left|\psi_i^B\right\rangle \left\langle \psi_k^B\right| , \quad \rho_{ik} = \sum_m c_{mi} c^*_{mk}, \tag{51}$$

$$\hat{\varrho}_{Z,A} = \sum_{i} \rho_{ii} \left|\psi_i^A\right\rangle \left\langle \psi_i^A\right| , \quad \rho_{ii} = \sum_m c_{mi} c^*_{mi}, \tag{52}$$

$$\hat{\varrho}_{Z,B} = \sum_{ik} \rho_{ik} \left|\psi_i^B\right\rangle \left\langle \psi_k^B\right| , \quad \rho_{ik} = \sum_m c_{mi} c^*_{mk}. \tag{53}$$

The characteristic equation for the matrix in Eq. (47) is

$$\lambda^3(\lambda - |C_1|^2 - |C_2|^2 - |C_3| - |C_4|) = 0, \tag{54}$$

and the eigenvalues $\lambda_{1,2} = 0, 1$. For the projected matrix $\hat{\varrho}_{Z,AB}$,

$$\lambda^2(\lambda - |C_1|^2 - |C_2|^2)(\lambda - |C_3|^2 - |C_4|^2) = 0, \tag{55}$$

we deduce $\lambda_{1,2} = 0$, $\lambda_3 = |C_1|^2 + |C_2|^2$, and $\lambda_4 = |C_3|^2 + |C_4|^2$. We apply a similar procedure to the other postmeasurement density matrices $\hat{\varrho}_{X,AB}$ and transformed coefficients $C^{(\Phi)}$.

For the reduced matrices in Eqs. (50), (51), and (53) the solutions are given by

$$\lambda_{1,2} = \tfrac{1}{2}[1 \pm \sqrt{1 - 4|C_1C_4 - C_2C_3|^2}], \tag{56}$$

and for the density matrix equation (52),

$$\lambda_1 = |C_1|^2 + |C_2|^2, \quad \lambda_2 = |C_3|^2 + |C_4|^2. \tag{57}$$

We introduce the function

$$h(x) = -x \log_2 x - (1 - x) \log_2 (1 - x). \tag{58}$$

The pairs of distinct roots of the characteristic polynomials of the entire and reduced density matrices satisfy the condition $\lambda_1 + \lambda_2 = 1$. It is easy to see that $h(x) = h(1 - x)$; therefore $h(\lambda_1) = h(\lambda_2)$, and we can use either of them to calculate the entropy.

The entropies corresponding to the bipartite and reduced density operators read

$$S(\hat{\varrho}_{AB}) = h(0) = 0, \tag{59}$$

$$S(\hat{\varrho}_A) = S(\hat{\varrho}_B) = h(\lambda), \tag{60}$$

$$S(A|B) = -h(\lambda). \tag{61}$$

The entropy corresponding to the bipartite density operator is zero meaning that the system is in the pure state. According to Eq. (54), $\lambda = \frac{1}{2}[1 \pm \sqrt{1 - 4|C_1C_4 - C_2C_3|^2}]$. For postmeasurement operators, after measuring the z projection of the spin A, expressions of the entropies read

$$S(\hat{\varrho}_{Z,AB}) = h(\mu), \tag{62}$$

$$S(\hat{\varrho}_{Z,B}) = h(\lambda), \tag{63}$$

$$S(Z|B) = h(\mu) - h(\lambda), \tag{64}$$

where

$$\mu = |C_1|^2 + |C_2|^2, \tag{65}$$

$$\lambda = \tfrac{1}{2}[1 + \sqrt{1 - 4|C_1C_4 - C_2C_3|^2}]. \tag{66}$$

After measuring the X component of the spin A, the entropies of the postmeasurement density operators read

$$S(\hat{\varrho}_{X,AB}) = h(\xi), \tag{67}$$

$$S(\hat{\varrho}_{X,B}) = h(\zeta), \tag{68}$$

$$S(X|B) = h(\xi) - h(\zeta). \tag{69}$$

Here, we introduced notations

$$\xi = |C_1^{(\Phi)}|^2 + |C_2^{(\Phi)}|^2, \tag{70}$$

$$\zeta = \tfrac{1}{2}\big[1 + \sqrt{1 - 4\big|C_1^{(\Phi)}C_4^{(\Phi)} - C_2^{(\Phi)}C_3^{(\Phi)}\big|^2}\big]. \tag{71}$$

The coefficients $C_i^{(\Phi)}$ are given by Eqs. (E2)–(E5), and the eigenvalues ξ and ζ are found through the original coefficient C_i. For more details we refer the reader to Appendix E [see Eqs. (E6)–(E8)]. Inserting all these expressions into Eq. (44), we obtain the following form of the inequality:

$$h(\xi) - h(\zeta) + h(\mu) \geqslant \log_2(1/c), \tag{72}$$

or

$$\begin{aligned} &-\xi \log_2 \xi - (1 - \xi) \log_2 (1 - \xi) \\ &\quad + \zeta \log_2 \zeta + (1 - \zeta) \log_2 (1 - \zeta) \\ &\quad - \mu \log_2 \mu - (1 - \mu) \log_2 (1 - \mu) \geqslant \log_2(1/c). \end{aligned} \tag{73}$$

The spatial inversion $\mathbb{R}^2$: $(x' = -x,\ y' = -y)$ in the polar coordinates $(x = \rho \cos\varphi,\ y = \rho \sin\varphi)$ is equivalent to the translation on the angle π, i.e., $(x' = \rho \cos(\varphi + \pi),\ y' = \rho \sin(\varphi + \pi))$ and is equivalent to $\rho \to -\rho$. Because of the

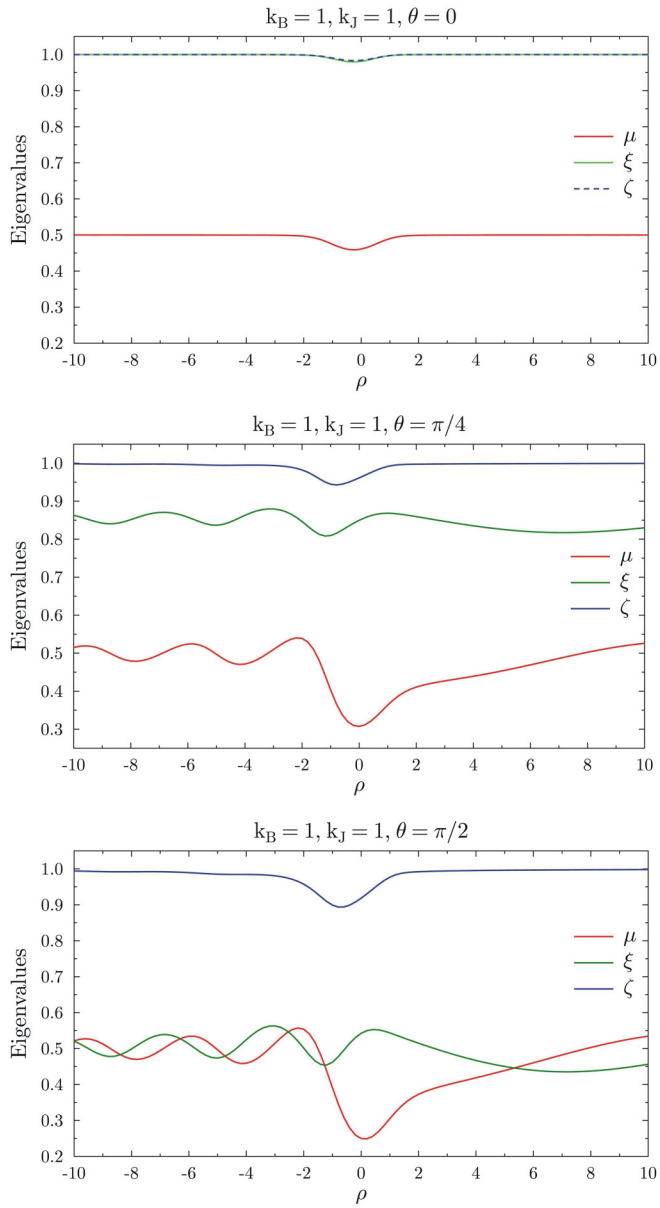

FIG. 2. The eigenvalues μ, ξ, and ζ of the postmeasurement density matrices $\varrho_{Z,AB}$, $\varrho_{X,AB}$, and $\varrho_{X,B}$, respectively, expressed by Eqs. (65), (70), and (71). The asymmetry between $-\rho$ and ρ results is related to the SO coupling, broken inversion symmetry, and $\varphi = \pi/4$.

spin-orbit (SO) coupling and broken inversion symmetry, we expect to see the difference between the results plotted for ρ and $-\rho$. We calculate the eigenvalues μ, ζ, and ξ numerically for different values of k, k_B, and k_J. Figure 2 represents the dependence of μ, ζ, and ξ on ρ for $k = 1$, $k_B = 1$, $k_J = 1$, $\varphi = \pi/4$, and different values of θ. These eigenvalues are important for the effect of quantum memory. In Fig. 3 we plotted the left-hand side, $S(X|B) + S(Z|B)$ (solid lines), and the right-hand side, $\log_2(1/c) + S(A|B)$ (dotted lines), of Eq. (44) for different values of the angle θ [$\mathbf{k} = (k\cos\theta, k\sin\theta, 0)$] and $k_B = 0$, $k_J = 1.0$, and $\varphi = \pi/4$. We note that the left-hand side of Eq. (44) quantifies the uncertainty of measurements, and the right-hand side quantifies the

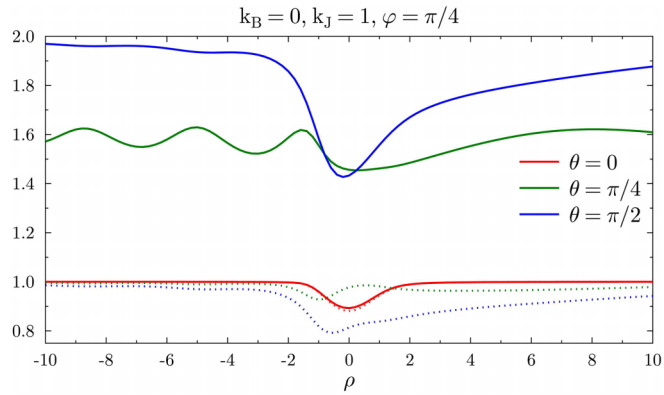

FIG. 3. The left-hand side (solid lines) and right-hand side (dotted lines) of Eq. (44) as a function of the distance between electrons ρ for $k_B = 0$ and different values of θ. The same color corresponds to the same set of parameters. The results for negative $-\rho$ are equivalent to the spatial inversion $\varphi \to \varphi + \pi$. The distance between electrons is calculated in units of the confinement length $\rho = |r|/l_B$ (where l_B is the magnetic confinement length).

minimal possible threshold value of the uncertainty. When the right-hand side is reduced because of the negative conditional quantum entropy $S(A|B) < 0$, the left-hand side also can be reduced without violation of the inequality in Eq. (44). We see in Fig. 3 that the right-hand side's minimum always coincides with the left-hand side's minimum. The left-hand side (solid lines) is always larger than the right-hand side, meaning that Eq. (44) holds. Reduction of the measurement uncertainty $S(X|B) + S(Z|B)$ is the essence of the quantum memory. As we see in the case $\theta = 0$ the right-hand side almost coincides with the left-hand side meaning that the measurement uncertainty is minimal and the effect of the quantum memory is most efficient in this case. The same tendency is even more pronounced in the case of a nonzero applied magnetic field $k_B = B/v = 1$; see Figs. 4 and 5. We

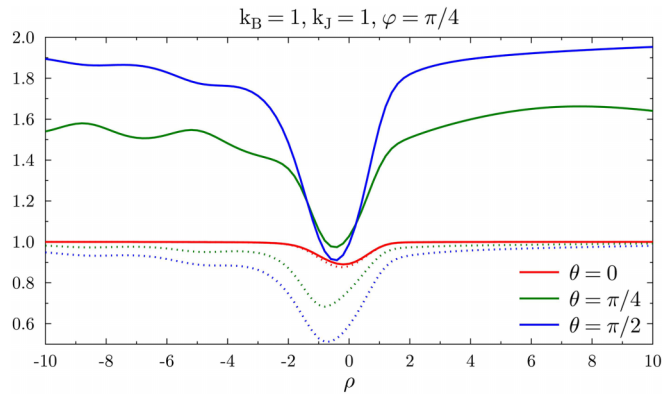

FIG. 4. The left-hand side (solid lines) and right-hand side (dotted lines) of Eq. (44) as a function of the distance between electrons ρ for $k_B = 1$. The same color corresponds to the same set of parameters. The results for negative $-\rho$ are equivalent to the spatial inversion $\varphi \to \varphi + \pi$. The distance between electrons is calculated in units of the confinement length $\rho = |r|/l_B$ (where l_B is the magnetic confinement length).

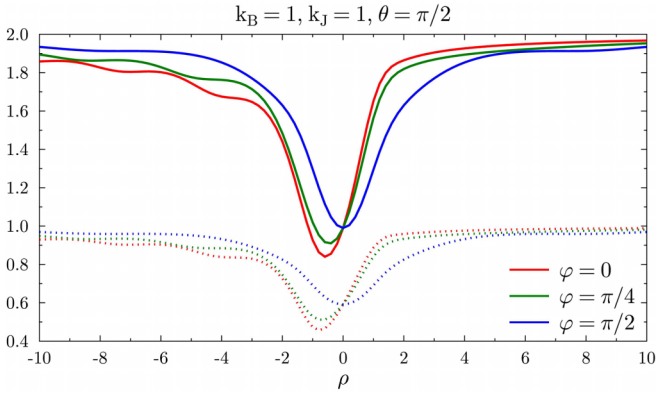

FIG. 5. The left-hand side (solid lines) and right-hand side (dotted lines) of Eq. (44) as a function of the distance between electrons ρ for $k_B = 1$ and $\theta = \pi/2$. The same color corresponds to the same set of parameters. The results for negative $-\rho$ are equivalent to the spatial inversion $\varphi \to \varphi + \pi$. The distance between electrons is calculated in units of the confinement length $\rho = |r|/l_B$ (where l_B is the magnetic confinement length).

see that the quantum memory decays sharply for $\rho > 2l_B$. On the other hand, the conditional quantum entropy $S(A|B)$ tends to zero asymptotically for large values of $\rho \gg l_B$. The asymmetry between $-\rho$ and ρ results is related to the SO coupling and broken inversion symmetry. In order to analyze the slow decay of the conditional quantum entropy, we exploit the definition of concurrence [29], $\mathcal{C} = |\langle\psi|\hat{\sigma}_y \otimes \hat{\sigma}_y |\psi^*\rangle|$, where $\hat{\sigma}_y \otimes \hat{\sigma}_y$ is the direct product of Pauli matrices, and calculate the entanglement between two electrons after scattering:

$$\mathcal{C} = \frac{2}{C_0^2}|C_2^*(\rho,\varphi)C_3^*(\rho,\varphi) - C_1^*(\rho,\varphi)C_4^*(\rho,\varphi)|. \tag{74}$$

As we see from Eq. (74), entanglement in the system is zero if at least two coefficients $C_n(\rho,\varphi)$ are zero. The same applies to $S(A|B)$. The conditional quantum entropy of the disentangled state is zero too. For further insights we rewrite Eq. (8) in the following equivalent form:

$$\alpha\beta\begin{pmatrix} C_1(\rho,\varphi) \\ C_2(\rho,\varphi) \\ C_3(\rho,\varphi) \\ C_4(\rho,\varphi) \end{pmatrix} = k_J \begin{pmatrix} e^{-i\theta} & 0 & 1 & 0 \\ 0 & -2 & 0 & 0 \\ 1 & 0 & e^{-i\theta} & 0 \\ 0 & 0 & 0 & -2 \end{pmatrix} \begin{pmatrix} A'_0(\rho,\varphi) \\ A'_1(\rho,\varphi) \\ A'_{0B}(\rho,\varphi) \\ A'_{1B}(\rho,\varphi) \end{pmatrix} + \begin{pmatrix} 2\pi e^{-i\theta} \\ 0 \\ 2\pi \\ 0 \end{pmatrix}. \tag{75}$$

Here, we introduced the notations $\alpha = C_0 e^{-i\theta}$, $\beta = e^{-ik\rho\cos\varphi}$, $A'_0(\rho,\varphi) = \beta k A_0(\rho,\varphi)$, $A'_1(\rho,\varphi) = \beta k A_1(\rho,\varphi)$, $A'_{0B}(\rho,\varphi) = \beta(k - 2k_B)A_{0B}(\rho,\varphi)$, and $A'_{1B}(\rho,\varphi) = \beta(k - 2k_B)A_{1B}(\rho,\varphi)$. As we see from Eqs. (74) and (75), when all A coefficients are zero, $\rho \gg |\mathbf{r}|/l_B$, only two coefficients, $C_1(\rho,\varphi)$ and $C_3(\rho,\varphi)$, are nonzero. Concurrence is zero, meaning that we have the trivial disentangled state. The numerical calculation results of coefficients A are shown in Fig. 6. We see that the values of coefficients A are finite even at distances of the order of $\rho = 10$. Thus the entanglement in the system is quite robust, and the system becomes disentangled only in the $\rho \gg 1$ limit. On the other hand, the effect of the quantum memory is more subtle and is pronounced only on distances not larger than $2l_B$. The dependence of the quantum memory on the distance between the itinerant and localized electrons is distinct compared with the improved uncertainty relations for the momentum and coordinate operators. The distance between the incident (itinerant) electron and target (localized in the quantum dot) electron in the experiment is smaller for larger momentum $\mathbf{p} = \hbar\mathbf{k}$ of the itinerant electron. However, the momentum and coordinate operators' uncertainty increases with $\mathbf{k}$. Quantum memory substantially reduces the uncertainties of spin measurements at the short distance between electrons.

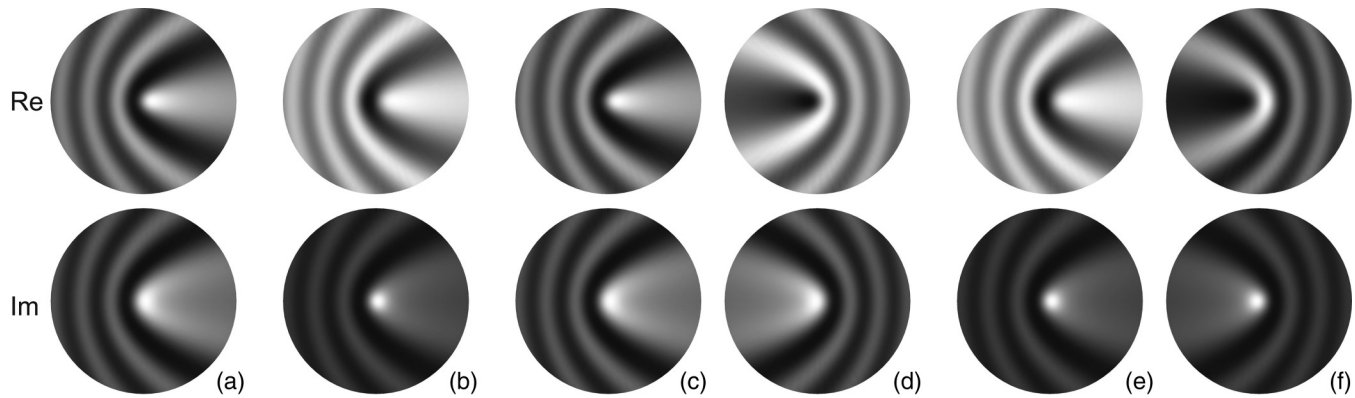

FIG. 6. The grayscale xy plots of real (upper row) and imaginary (lower row) parts of the coefficients: (a) A'_0, (b) A'_1, (c) A'_{0B} for $k_B = 0$, (d) A'_{0B} for $k_B = 0$, (e) A'_{1B} for $k_B = 0$, and (f) A'_{1B} for $k_B = 1$. The plots include the region of $\rho = |\mathbf{r}|/l_B \leqslant 10$ around the center of the quantum dot, where l_B is the magnetic confinement length. Black and white correspond to the minimal and maximal values, respectively. The coefficients decay to zero for $\rho \gg 1$ (not shown).

V. CONCLUSIONS

It is well known that measurements performed on quantum systems are specific and may be invasive and destroy the state of interest. Beyond that, quantumness limits the accuracy of measurements due to the fundamental uncertainty relations. On the other hand, quantum correlations and memory might reduce quantum measurements' uncertainty. We studied two types of measurements performed on a topological system: (a) measurements performed on the spin operators and (b) measurements of the canonical pair of operators, namely, the momentum and the coordinate. We quantified the spin operator's measurements through the entropic measures of uncertainty and exploited the concept of quantum memory. For the momentum and coordinate operators, we exploited the improved uncertainty relations. We showed that the dependence of the quantum memory on the distance between the itinerant and localized electrons is distinct compared with the improved uncertainty relations for momentum and coordinate operators. While the momentum and coordinate operators' uncertainty increases with the momentum of the itinerant electron, the quantum memory reduces the uncertainty of spin measurements when the distance between electrons is not larger than several confinement lengths l_B. Therefore, based on the discovered effect, we propose an indirect measurement scheme for the momentum and coordinate operators through the spin operator. Due to the factor of quantum memory, such indirect measurements in topological insulators lead to smaller uncertainties than one has with direct measurements.

APPENDIX A: COEFFICIENTS OF THE WAVE FUNCTION

$$A_0(\mathbf{r}) = \int \rho' d\rho' d\varphi' \, K_0(-iE|\mathbf{r}-\mathbf{r}'|/v)|\psi_D(\rho')|^2 e^{ik\rho'\cos\varphi'}, \tag{A1}$$

$$A_1(\mathbf{r}) = \int \rho' d\rho' d\varphi' \, K_1(-iE|\mathbf{r}-\mathbf{r}'|/v)|\psi_D(\rho')|^2 e^{ik\rho'\cos\varphi'}, \tag{A2}$$

$$A_{0B}(\mathbf{r}) = \int \rho' d\rho' d\varphi' \, K_0(-i(E-2B)|\mathbf{r}-\mathbf{r}'|/v) \times |\psi_D(\rho')|^2 e^{ik\rho'\cos\varphi'}, \tag{A3}$$

$$A_{1B}(\mathbf{r}) = \int \rho' d\rho' d\varphi' \, K_1(-i(E-2B)|\mathbf{r}-\mathbf{r}'|/v) \times |\psi_D(\rho')|^2 e^{ik\rho'\cos\varphi'}. \tag{A4}$$

The explicit forms of the matrix elements are

$$\begin{aligned}
\hat{V}_{00}(\mathbf{r}_A) &= \langle\psi_{D,0}(\mathbf{r}_B)|\hat{V}|\psi_{D,0}(\mathbf{r}_B)\rangle = \langle\psi_{D,0}(\mathbf{r}_B)|J\hat{\sigma}_A\hat{\sigma}_B\delta(\mathbf{r}_A-\mathbf{r}_B)|\psi_{D,0}(\mathbf{r}_B)\rangle = J|\psi_D(\mathbf{r}_A)|^2\hat{\sigma}_A^z,\\
\hat{V}_{01}(\mathbf{r}_A) &= \langle\psi_{D,0}(\mathbf{r}_B)|\hat{V}|\psi_{D,1}(\mathbf{r}_B)\rangle = \langle\psi_{D,0}(\mathbf{r}_B)|J\hat{\sigma}_A\hat{\sigma}_B\delta(\mathbf{r}_A-\mathbf{r}_B)|\psi_{D,1}(\mathbf{r}_B)\rangle = J|\psi_D(\mathbf{r}_A)|^2\left(\hat{\sigma}_A^x - i\hat{\sigma}_A^y\right),\\
\hat{V}_{10}(\mathbf{r}_A) &= \langle\psi_{D,1}(\mathbf{r}_B)|\hat{V}|\psi_{D,0}(\mathbf{r}_B)\rangle = \langle\psi_{D,1}(\mathbf{r}_B)|J\hat{\sigma}_A\hat{\sigma}_B\delta(\mathbf{r}_A-\mathbf{r}_B)|\psi_{D,0}(\mathbf{r}_B)\rangle = J|\psi_D(\mathbf{r}_A)|^2\left(\hat{\sigma}_A^x + i\hat{\sigma}_A^y\right),\\
\hat{V}_{11}(\mathbf{r}_A) &= \langle\psi_{D,1}(\mathbf{r}_B)|\hat{V}|\psi_{D,1}(\mathbf{r}_B)\rangle = \langle\psi_{D,1}(\mathbf{r}_B)|J\hat{\sigma}_A\hat{\sigma}_B\delta(\mathbf{r}_A-\mathbf{r}_B)|\psi_{D,1}(\mathbf{r}_B)\rangle = -J|\psi_D(\mathbf{r}_A)|^2\hat{\sigma}_A^z.
\end{aligned} \tag{A5}$$

APPENDIX B: APPROXIMATING INTEGRALS

We utilize the following asymptotic expressions for the Bessel functions at $z \gg 1$:

$$K_{l=0,1}(z) = \frac{\pi}{2z}e^{-z}\left\{1 + \frac{4l^2-1}{8z}\right\}, \tag{B1}$$

$z = -ik_{(B)}|\mathbf{r}-\mathbf{r}'| = -ik_{(B)}\sqrt{\rho^2+\rho'^2-2\rho\rho'\cos(\varphi-\varphi')}$, and $k_{(B)} = \frac{E-(2B)}{v} = k - (2B/v)$. We apply these asymptotic expressions to Eqs. (A1) and (A2):

$$A_{l=0,1(B)}(\vec{r}) \approx \int \rho' d\rho' d\gamma |\psi_D(\rho')|^2 e^{ik\rho'\cos(\gamma+\varphi)}\frac{\pi}{2z}e^{-z}\left(1 + \frac{4l^2-1}{8z}\right), \tag{B2}$$

where $\gamma = \varphi' - \varphi$ is the scattering angle. We express z as $z = -ik_{(B)}a\sqrt{1-b\cos\gamma}$, where $a = \sqrt{\rho^2+\rho'^2}$ and $b = 2\rho\rho'/a^2$. Assuming that b is a small parameter, we expand the square root into a power series and retain only the leading-order terms. Performing an integration over the angle γ, we calculate the following integral:

$$I_\gamma = -\int_0^{2\pi} d\gamma \exp\left[ik\rho'\cos(\gamma+\varphi) + ik_{(B)}a\left(1-\frac{b}{2}\cos\gamma\right)\right]\left[\frac{1}{ik_{(B)}a}\frac{1}{(1-\frac{b}{2}\cos\gamma)} + \frac{4l^2-1}{8k_{(B)}^2a^2}\frac{1}{(1-b\cos\gamma)}\right]. \tag{B3}$$

Both integrals in this expression can be transformed into contour integrals along a circle of unit radius around the origin: Assuming $z = e^{i\gamma}$, $d\gamma = (1/i)dz/z$, and $\cos\gamma = (1/2)(z+1/z)$, we deduce

$$\int_{|z|=1} dz \frac{f(z)}{2z - cz^2 - c}. \tag{B4}$$

Here, c is either b or $b/2$. The square polynomial in the denominator has two real roots:

$$z_{1,2} = \frac{1}{c}[1 \pm \sqrt{1-c^2}]. \tag{B5}$$

Only the root with the minus sign is located inside the unit circle at $z_0 \approx c/2e$ and $\arg z_0 = 0$, and both residuals are equal to -1. The final form of Eq. (B3) reads

$$I_\gamma = \pi \frac{-8ik_{(B)}a + 4l^2 - 1}{4k_{(B)}^2 a^2} \exp[ik\rho' \cos\varphi + ik_{(B)}a(1-b/2)], \tag{B6}$$

and

$$A_{l=0,1(B)}(\vec{r}) = \frac{\pi}{4l_B^2} \int \rho' d\rho' \frac{-8ik_{(B)}\sqrt{\rho^2+\rho'^2} + 4l^2 - 1}{k_{(B)}^2(\rho^2+\rho'^2)} \exp\left[\frac{-\rho'^2}{l_B^2} + ik\rho' \cos\varphi + ik_{(B)} \frac{\rho^2+\rho'^2-\rho\rho'}{\sqrt{\rho^2+\rho'^2}}\right]. \tag{B7}$$

Introducing the notation $x = \rho'/\rho$, we rewrite the expression as follows:

$$\begin{aligned} A_{l=0,1(B)}(\vec{r}) &= \frac{\pi}{4l_B^2} \int x dx \frac{-8ik_{(B)}\rho\sqrt{1+x^2} + 4l^2 - 1}{k_{(B)}^2\rho^2(1+x^2)} \exp\left[-\left(\frac{\rho}{l_B}\right)^2 x^2 + ik\rho x \cos\varphi + ik_{(B)}\rho \frac{1-x+x^2}{\sqrt{1+x^2}}\right] \\ &\approx \frac{\pi}{4l_B^2} \frac{1}{k_{(B)}^2\rho^2} \int x dx[(4ik_{(B)}\rho - 4l^2 + 1)x^2 - (8ik_{(B)}\rho - 4l^2 + 1)] \\ &\quad \times \exp\left[-\left(\frac{\rho^2}{l_B^2} + \frac{3i}{2}\right)x^2 + i(k\cos\varphi - k_{(B)})\rho x + ik_{(B)}\rho\right]. \end{aligned} \tag{B8}$$

In the next step we analyze the term proportional to x^3. Considering that $\rho^2/l_B^2 \gg 1$, we perform the integration over x and obtain

$$A_{l=0,1}(\vec{r}) \approx \frac{\pi}{8(k_{(B)}l_B)} \frac{8ik_{(B)}\rho - 4l^2 + 1}{(k_{(B)}\rho)^3} k_{(B)}^2 e^{ik_{(B)}\rho}\left[1 + \sqrt{\pi} i\kappa_{(B)} l_B[1 + \mathrm{erf}(i\kappa_{(B)}l_B)]e^{-\kappa^2 l_B^2}\right], \tag{B9}$$

where $\kappa_{(B)} = (k\cos\varphi - k_B)/2$. Noting that the last line in Eq. (B9) is a function of φ, we expand it in terms of the small parameter $l_B\kappa_{(B)} \ll 1$:

$$\begin{aligned} 1 + \sqrt{\pi} i\kappa_{(B)} l_B[1 + \mathrm{erf}(i\kappa_{(B)}l_B)]e^{-\kappa^2 l_B^2} &\approx 1 + i\sqrt{\pi}\kappa_{(B)}l_B - 2(\kappa_{(B)}l_B)^2 = 1 - \frac{k_{(B)}^2 l_B^2}{2} \\ &\quad - \frac{i\sqrt{\pi}}{2} k_{(B)} l_B + \left(\frac{i\sqrt{\pi}}{2} + k_{(B)}l_B\right) k l_B \cos\varphi - \frac{1}{2}k^2 l_B^2 \cos^2\varphi. \end{aligned} \tag{B10}$$

APPENDIX C: EXPRESSIONS OF INTEGRALS INTEGRATED OVER THE ANGLE

After integration over the angular variable φ, from Eq. (26) we deduce

$$I_{00}^{\varphi} = \frac{19\pi}{16}k^4 + \left(\frac{3}{4}\pi - 1\right)\pi k^2 + 2\pi, \tag{C1}$$

$$\begin{aligned} I_{BB}^{\varphi} &= I_{00}^{\varphi} + 8\pi k_B^4 - 16\pi k k_B^3 + (14k^2 + 2\pi - 8)\pi k_B^2 \\ &\quad + [(8-2\pi)k - 6k^3]\pi k_B, \end{aligned} \tag{C2}$$

$$\begin{aligned} I_{0B}^{\varphi} &= I_{00}^{\varphi} - (4-k^2)\pi k_B^2 - [3k^2 + (\pi-4)]\pi k k_B \\ &\quad -2i\pi\sqrt{\pi}\left[k k_B^2 - \left(\frac{5}{4}k^2 - 1\right)k_B\right], \end{aligned} \tag{C3}$$

$$I_{B0}^{\varphi} = \left(I_{0B}^{\varphi}\right)^*. \tag{C4}$$

The difference between Eqs. (C1) and (C2) vanishes when $k_B = 0, k$, and the expressions become symmetric with respect to $k_B = 0.5k$ (Fig. 7).

APPENDIX D: NORMALIZATION OF THE WAVE FUNCTION

We calculate integrals for the products of the functions $f_{\lambda b}$ used in the normalization of the wave function:

$$\begin{aligned} I^N_{\lambda_1\lambda_2 b_1 b_2} &= \int_1^\infty \rho d\rho f^*_{\lambda_1 b_1}(\rho) f_{\lambda_2 b_2}(\rho) = \left[\frac{\pi}{k_{b_1}k_{b_2}}\right]^2 \\ &\quad \times \sum_{n=2}^{4} G_n i^{n-1}(-i\Delta k_{(b)})^n \Gamma(-n, -i\Delta k_{(b)}), \end{aligned} \tag{D1}$$

where

$$G_2 = k_{b_1}k_{b_2}, \tag{D2}$$

$$G_3 = \frac{1}{8}\left(\lambda_1 k_{b_2} - \lambda_2 k_{b_1}\right), \tag{D3}$$

$$G_4 = \frac{\lambda_1\lambda_2}{64}. \tag{D4}$$

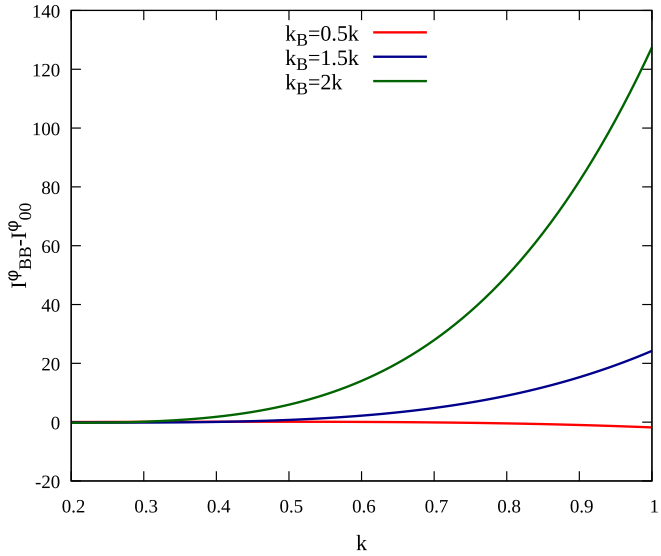

FIG. 7. Difference $I^{\varphi}_{BB} - I^{\varphi}_{00}$ as a function of k for different proportionality coefficients of k_B relative to k.

Expressions for all possible combinations of the parameters read

$$I^{N}_{00,00} = \frac{\pi^2}{2k^4}\left(k^2 + \frac{1}{128}\right), \tag{D5}$$

$$I^{N}_{11,00} = \frac{\pi^2}{2k^4}\left(k^2 + \frac{9}{128}\right), \tag{D6}$$

$$I^{N}_{00,BB} = \frac{\pi^2}{(k-2k_B)^4}\left((k-2k_B)^2 + \frac{1}{128}\right), \tag{D7}$$

$$I^{N}_{11,BB} = \frac{\pi^2}{(k-2k_B)^4}\left((k-2k_B)^2 + \frac{9}{128}\right), \tag{D8}$$

$$I^{N}_{10,00} = \frac{\pi^2}{2k^4}\left(k^2 - \frac{3}{128} + \frac{1}{3}ik\right), \tag{D9}$$

$$I^{N}_{01,00} = \left(I^{N}_{10,00}\right)^{*}, \tag{D10}$$

$$I^{N}_{10,BB} = \frac{\pi^2}{2(k-2k_B)^4}\left((k-2k_B)^2 - \frac{3}{128} + \frac{1}{3}i(k-2k_B)\right), \tag{D11}$$

$$I^{N}_{01,BB} = \frac{\pi^2}{2(k-2k_B)^4}\left((k-2k_B)^2 - \frac{3}{128} - \frac{1}{3}i(k-2k_B)\right). \tag{D12}$$

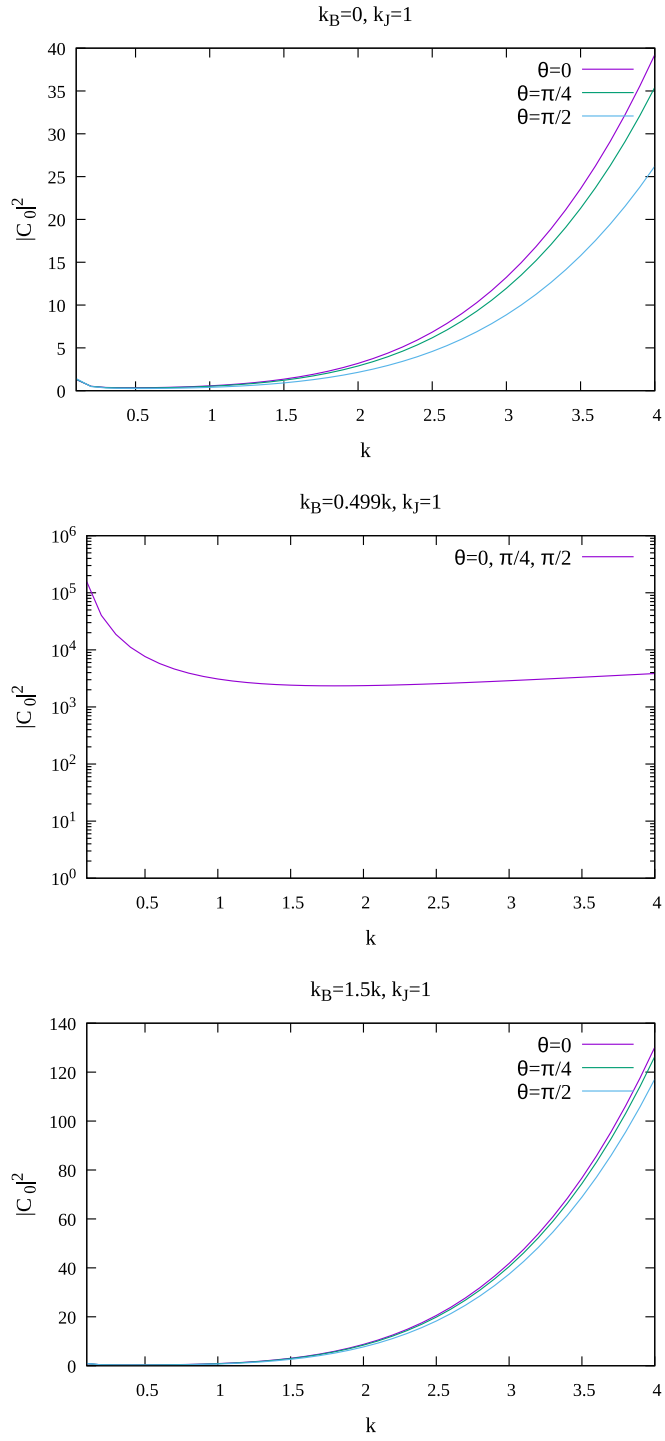

FIG. 8. The dependence of $|C_0|^2$ on k given in Eq. (D14) and plotted for several values of k_B and θ for $k_J = k$. The function has a singularity when k_B approaches $0.5k$.

Squares of the modules of the coefficients are as follows:

$$\int |C_1|^2 = A(k_J k)^2 I^{\varphi}_{00}\left(I^{N}_{00,00} + I^{N}_{11,00} + I^{N}_{01,00}e^{i\theta} + I^{N}_{10,00}e^{-i\theta}\right) = AI^{\varphi}_{00}\frac{(\pi k_J)^2}{k^2}\left[k^2(1+\cos\theta) + \frac{1}{128}(10 - 3\cos\theta) + \frac{1}{3}\sin\theta\right], \tag{D13}$$

where $A = |\psi_D(\rho')|^2/(8\pi^2)$ includes the rest of the normalization terms in front of the parentheses. The calculation of $|C_2|^2$ and $|C_4|^2$ is rather straightforward. The expression for $|C_3|^2$ is different from Eq. (D13) only in terms of the sign in front of the $\sin\theta$ term. Finally, the normalization coefficient reads

$$|C_0|^2 = \int \sum_{i=1}^{4} |C_i|^2 = 2A(\pi k_J)^2 \times \left[\frac{I_{00}^{\varphi}}{k^2}\left(k^2(1+\cos\theta) + \frac{1}{128}(10 - 3\cos\theta)\right) + \frac{I_{BB}^{\varphi}}{(k-2k_B)^2}\left((k-2k_B)^2 + \frac{5}{64}\right)\right]. \tag{D14}$$

One can see that the norm diverges at $k = 0$ and $k_B = 0.5k$. The dependence of $|C_0|^2$ on k is plotted in Fig. 8.

APPENDIX E: COEFFICIENTS IN THE NEW BASIS

The coefficients of the alternative representation of the wave function in the basis $\{\phi_1, \phi_2\}$ are as follows:

$$|\Phi\rangle_{AB} = C_1^{(\Phi)}\left|\phi_1^A\phi_1^B\right\rangle + C_2^{(\Phi)}\left|\phi_1^A\phi_2^B\right\rangle + C_3^{(\Phi)}\left|\phi_2^A\phi_1^B\right\rangle + C_4^{(\Phi)}\left|\phi_2^A\phi_2^B\right\rangle, \tag{E1}$$

where

$$C_1^{(\Phi)} = \tfrac{1}{2}(C_1 + C_2 + C_3 + C_4), \tag{E2}$$

$$C_2^{(\Phi)} = \tfrac{1}{2}(C_1 - C_2 + C_3 - C_4), \tag{E3}$$

$$C_3^{(\Phi)} = \tfrac{1}{2}(C_1 + C_2 - C_3 - C_4), \tag{E4}$$

$$C_4^{(\Phi)} = \tfrac{1}{2}(C_1 - C_2 - C_3 + C_4). \tag{E5}$$

One can show that

$$\left|C_1^{(\Phi)}\right|^2 + \left|C_2^{(\Phi)}\right|^2 = \tfrac{1}{2}[1 + (C_1C_3^* + C_1^*C_3) + (C_2C_4^* + C_2^*C_4)], \tag{E6}$$

$$\left|C_3^{(\Phi)}\right|^2 + \left|C_4^{(\Phi)}\right|^2 = \tfrac{1}{2}[1 - (C_1C_3^* + C_1^*C_3) - (C_2C_4^* + C_2^*C_4)], \tag{E7}$$

$$C_1^{(\Phi)}C_4^{(\Phi)} - C_2^{(\Phi)}C_3^{(\Phi)} = C_1C_4 - C_2C_3. \tag{E8}$$

[1] A. Messiah, *Quantum Mechanics* (Dover, Mineola, NY, 2014).

[2] P. J. Coles, M. Berta, M. Tomamichel, and S. Wehner, Entropic uncertainty relations and their applications, Rev. Mod. Phys. **89**, 015002 (2017).

[3] L. Maccone and A. K. Pati, Stronger uncertainty relations for all incompatible observables, Phys. Rev. Lett. **113**, 260401 (2014).

[4] M. Berta, M. Christandl, R. Colbeck, J. M. Renes, and R. Renner, The uncertainty principle in the presence of quantum memory, Nat. Phys. **6**, 659 (2010).

[5] D. Wang, F. Ming, M.-L. Hu, and L. Ye, Quantum-memory-assisted entropic uncertainty relations, Ann. Phys. (Berlin) **531**, 1900124 (2019).

[6] F. Ming, D. Wang, X.-G. Fan, W.-N. Shi, L. Ye, and J.-L. Chen, Improved tripartite uncertainty relation with quantum memory, Phys. Rev. A **102**, 012206 (2020).

[7] H. Dolatkhah, S. Haseli, S. Salimi, and A. S. Khorashad, Tightening the tripartite quantum-memory-assisted entropic uncertainty relation, Phys. Rev. A **102**, 052227 (2020).

[8] B. Bergh and M. Gärttner, Entanglement detection in quantum many-body systems using entropic uncertainty relations, Phys. Rev. A **103**, 052412 (2021).

[9] B.-F. Xie, F. Ming, D. Wang, L. Ye, and J.-L. Chen, Optimized entropic uncertainty relations for multiple measurements, Phys. Rev. A **104**, 062204 (2021).

[10] L. Chotorlishvili, A. Gudyma, J. Wätzel, A. Ernst, and J. Berakdar, Spin-orbit-coupled quantum memory of a double quantum dot, Phys. Rev. B **100**, 174413 (2019).

[11] M.-L. Song, L.-J. Li, X.-K. Song, L. Ye, and D. Wang, Environment-mediated entropic uncertainty in charging quantum batteries, Phys. Rev. E **106**, 054107 (2022).

[12] H. Zhu, Zero uncertainty states in the presence of quantum memory, npj Quantum Inf. **7**, 47 (2021).

[13] P. Kurashvili, L. Chotorlishvili, K. Kouzakov, and A. Studenikin, Quantum spin-flavour memory of ultrahigh-energy neutrino, Eur. Phys. J. Plus **137**, 234 (2022).

[14] P. Kurashvili, L. Chotorlishvili, K. A. Kouzakov, A. G. Tevzadze, and A. I. Studenikin, Quantum witness and invasiveness of cosmic neutrino measurements, Phys. Rev. D **103**, 036011 (2021).

[15] D. Sokolovski and E. Y. Sherman, Spin measurements and control of cold atoms using spin-orbit fields, Phys. Rev. A **89**, 043614 (2014).

[16] D. Sokolovski and E. Ya. Sherman, Measurement of noncommuting spin components using spin-orbit interaction, Phys. Rev. A **84**, 030101(R) (2011).

[17] O. V. Yazyev, J. E. Moore, and S. G. Louie, Spin polarization and transport of surface states in the topological insulators Bi_2Se_3 and Bi_2Te_3 from first principles, Phys. Rev. Lett. **105**, 266806 (2010).

[18] T. S. Seifert, S. Kovarik, P. Gambardella, and S. Stepanow, Accurate measurement of atomic magnetic moments by minimizing the tip magnetic field in STM-based electron paramagnetic resonance, Phys. Rev. Res. **3**, 043185 (2021).

[19] P. Willke, A. Singha, X. Zhang, T. Esat, C. P. Lutz, A. J. Heinrich, and T. Choi, Tuning single-atom electron spin resonance in a vector magnetic field, Nano Lett. **19**, 8201 (2019).

[20] F. Baruffa, P. Stano, and J. Fabian, Spin-orbit coupling and anisotropic exchange in two-electron double quantum dots, Phys. Rev. B **82**, 045311 (2010).

[21] G. Cordourier-Maruri, Y. Omar, R. de Coss, and S. Bose, Graphene-enabled low-control quantum gates between static and mobile spins, Phys. Rev. B **89**, 075426 (2014).

[22] S. Wolski, M. Inglot, C. Jasiukiewicz, K. A. Kouzakov, T. Masłowski, T. Szczepański, S. Stagraczyński, R. Stagraczyński,

V. K. Dugaev, and L. Chotorlishvili, Random spin-orbit gates in the system of a topological insulator and a quantum dot, Phys. Rev. B **106**, 224418 (2022).

[23] J. R. Taylor, *Scattering Theory: The Quantum Theory of Nonrelativistic Collisions* (Dover, Mineola, NY, 2006).

[24] A. Khelashvili and T. Nadareishvili, Generalized Heisenberg uncertainty relation in spherical coordinates, Int. J. Mod. Phys. B **36**, 2250072 (2022).

[25] P. Carruthers and M. M. Nieto, Phase and angle variables in quantum mechanics, Rev. Mod. Phys. **40**, 411 (1968).

[26] J. R. Lombardi, Hydrogen atom in the momentum representation, Phys. Rev. A **22**, 797 (1980).

[27] L. Chotorlishvili, P. Zięba, I. Tralle, and A. Ugulava, Zitterbewegung and symmetry switching in Klein's four-group, J. Phys. A: Math. Theor. **51**, 035004 (2018).

[28] M. M. Wilde, *Quantum Information Theory* (Cambridge University Press, Cambridge, 2013).

[29] W. K. Wootters, Entanglement of formation of an arbitrary state of two qubits, Phys. Rev. Lett. **80**, 2245 (1998).